Universal Validation of the GERT Local Thermodynamic Extension: Zero-Parameter Rotation Curve Predictions Across 191 Galaxies

V. P. Dutra *

Posted Date: 26 March 2026

doi: 10.20944/preprints202603.2170.v1

Keywords: GERT; dark matter; rotation curves; SPARC; RAR; zero-parameter model; MOND; Verlinde EG; early-type galaxies

 doi:10.20944/preprints202603.2170.v1

Article

Universal Validation of the GERT Local Thermodynamic Extension: Zero-Parameter Rotation Curve Predictions Across 191 Galaxies

V. P. Dutra

Independent Researcher (Chemistry), Institute of Chemistry, Federal University of Rio de Janeiro (UFRJ), Rio de Janeiro, RJ, Brazil; veronica.p.d@outlook.com

Abstract

Background: The Gibbs Energy Redistribution Theory (GERT) replaces dark matter and dark energy with thermodynamic functions of local density, derived from the Gibbs free energy criterion. Paper VI established a zero-parameter local extension validated on six SPARC galaxies, six clusters, and the Baryonic Tully-Fisher Relation, calibrated solely against CMB, BAO, and Type Ia data. *Methods:* We apply the identical GERT v0.4 equation — without modification — to the complete SPARC database: 175 late-type (LTG) and 16 early-type galaxies (ETG), spanning 10^7–10^{11} $M_\odot$ across all morphological types. *Results:* GERT improves over Newtonian baryons in 165/175 LTGs (94.3%) and all 16 ETGs (100%). Across 3423 data points, RAR scatter falls from 0.308 to 0.212 dex (−31.4%) with zero free parameters. The 7% offset between $a_{\rm GERT} = cH_0/2\pi$ and Milgrom's a_0 is a quantitative target for the forthcoming pre-relativistic extension. *Conclusions:* A single thermodynamic equation, calibrated against cosmological probes alone, predicts galactic rotation curves across all morphologies, supporting a thermodynamic bridge from cosmic to galactic scales.

Keywords: GERT; dark matter; rotation curves; SPARC; RAR; zero-parameter model; MOND; Verlinde EG; early-type galaxies

---

Guidelines for Readers (Roadmap)

Position in the Gibbs Energy Redistribution Theory (GERT) series. This manuscript is Paper VII of the Gibbs Energy Redistribution Theory (GERT) series, currently comprising thirteen papers (Papers I–XIII). It is self-contained and does not presuppose knowledge of the companion works beyond Paper VI [1], whose zero-parameter equation is applied here without modification. The series is cumulative: all thermodynamic functions and frozen parameters used here are inherited from Paper I [2]. For a complete programme overview, see Table 1 of Paper I.

Predecessor papers. For orientation, the preceding six papers are:

- Paper I [2] establishes the thermodynamic ontology of GERT and calibrates the frozen functions against Cosmic Microwave Background (CMB), Baryon Acoustic Oscillations (BAO), and Type Ia supernovae (SNe Ia) data.
- Paper II [3] identifies the late-time hyperdilute boundary where relativistic metric legibility progressively dissolves.
- Paper III [4] determines the early-time emergence boundary, completing the finite relativistic domain map.
- Paper IV [5] reconstructs the internal thermodynamic anatomy of the relativistic window, including cohesive and entropic transition landmarks.
- Paper V [6] derives the gravitational-wave consequences of that anatomy, including the Thermodynamic Parsec.
- Paper VI [1] formulates the zero-parameter local bridge and validates it on six representative galaxies, six clusters, and the Baryonic Tully-Fisher Relation (BTFR).

 doi:10.20944/preprints202603.2170.v1

Structure of this manuscript. This manuscript is a strict full-sample validation: the same equation from Paper VI is applied to 191 galaxies without any adjustment. The seven stages of the argument are listed below.

To make the logic of this manuscript transparent from the first page, the roadmap below separates this article into seven operational stages, each with a distinct role in the argument. (Note: the term "Layer" is reserved throughout this paper for the GERT ontological stratigraphy of Papers I–VIII; the stages below are structural divisions of this manuscript only.)

Stage 1 — Physical Premise and Scope (Section 1). We define the open problem after Paper VI [1] and position this work as a strict full-sample validation of the same local equation, not a new branch of theory.

Stage 2 — Formal Framework and Frozen Inputs (Section 2). We restate the frozen thermodynamic functions, the v0.4 bridge equation, the density-based screening mechanism, and the deterministic Spitzer Photometry and Accurate Rotation Curves (SPARC) pipeline used without retuning.

Stage 3 — Galaxy-Scale Validation: Late-Type Galaxies (LTG) (Section 3). We test the model across 175 late-type galaxies (LTG), emphasizing per-galaxy goodness-of-fit and the Radial Acceleration Relation behaviour in low-density outer regions.

Stage 4 — Galaxy-Scale Validation: Early-Type Galaxies (ETG) (Section 4). We stress-test the same equation on 16 early-type galaxies (ETG), probing compact, bulge-dominated systems where acceleration-threshold alternatives are most constrained.

Stage 5 — Combined Performance and Theory Comparison (Section 5). We consolidate LTG+ETG statistics, evaluate global Radial Acceleration Relation (RAR) scatter reduction, and compare predictive status against Lambda Cold Dark Matter (ΛCDM), Modified Newtonian Dynamics (MOND), and Verlinde emergent gravity (Verlinde EG).

Stage 6 — Physical Interpretation and Falsifiability (Section 6). We interpret the 7% acceleration-scale offset, identify domain-specific failure modes, and state concrete observational tests that can falsify the bridge.

Stage 7 — Synthesis and Next Validation Frontier (Section 7). We separate what is established from what remains provisional and define the mandatory next checks for full programme closure in Paper VIII.

For reproducibility, all processing steps (datasets, scripts, and execution order) are documented in the Code and Data Availability Statement and in the script inventory included in the manuscript package.

1. Introduction

1.1. The Validation Gap

The Gibbs Energy Redistribution Theory (GERT) series [1] established the first zero-parameter local extension. The derivation demonstrated that the same thermodynamic functions $f_M(x)$ and $f_L(x)$ that govern cosmic evolution (Papers I–IV [2–6]) also govern the gravitational dynamics of bound systems, when evaluated at the local thermodynamic state variable $x_{\rm loc}(r) = \log_{10}[\rho_{\rm bar}(< r)]$ of the system rather than the cosmological background density.

The cosmological calibration used by the local extension is inherited from Paper I, constrained against cosmic microwave background, baryon acoustic oscillation, and Type Ia supernova (CMB/BAO/SN) datasets [2,7].

Paper VI [1] validated this extension against six representative Spitzer Photometry and Accurate Rotation Curves (SPARC) galaxies spanning the full stellar mass range (10^7–10^{11} $M_\odot$), six galaxy clusters, and the Baryonic Tully-Fisher Relation — all with zero free parameters. The declared open challenge at the close of Paper VI [1] was explicit: the six-galaxy sample constitutes a proof of concept. The definitive test requires application to the complete SPARC database — 175 late-type and 16 early-type galaxies — without any adjustment of the equation or its parameters.

This paper delivers that test.

 doi:10.20944/preprints202603.2170.v1

1.2. Four Competing Frameworks

The mass discrepancy in galaxies — the systematic excess of $g_{\rm obs}$ over $g_{\rm bar}$ — has generated four distinct theoretical frameworks, each with characteristic strengths and failures [8]. These are summarised in Table 1.

Table 1. Comparison of four theoretical frameworks for the dark matter problem.

Property	ΛCDM	MOND	Verlinde EG	GERT (this paper)
Dark matter substance	Yes (CDM particle)	No	No	No
Free parameters (local)	≥2 per galaxy	a_0 (postulated)	0	**0**
Cosmological background	Yes	No	Fails [9]	Yes (Paper I [2])
Rotation curves (6 galaxies)	With tuning	Yes	Yes	Yes (Paper VI [1])
Rotation curves (191 galaxies)	With tuning	Yes	80% [10]	**94.8% (0 params)**
RAR scatter (0-param)	Not applicable	Not applicable	0.200 dex [10]	**0.212 dex**
Galaxy clusters	Yes (with CDM)	Fails [11,12]	Fails [13,14]	Yes (Paper VI [1])
ETG validation	With tuning	Difficult	Unclear	**16/16 (100%)**
BTFR slope = 4	Empirical	By construction	Approx.	Derived (Paper VI [1])
Milgrom scale origin	Coincidence	Postulate	Asserts cH_0	**Derives** $cH_0/2\pi$
Threshold space	—	Acceleration	Acceleration	**Density**
Unified cosmic + local	No	No	No	**Yes**

The critical distinction of the GERT framework is its threshold space. Modified Newtonian Dynamics (MOND) and Verlinde emergent gravity (Verlinde EG) both use an acceleration threshold a_0: corrections become operative when $g_{\rm bar} \lesssim a_0$. GERT uses a **density threshold**: corrections become operative when $x_{\rm loc} \gtrsim \log \rho_{L2} = -23.93$. This distinction has observable consequences: GERT naturally predicts different behaviour in compact high-density galaxies versus diffuse systems with similar accelerations — a discrimination that is in principle measurable with high-resolution photometry.

At the framework level, MOND is usually discussed from its original non-relativistic formulation to its relativistic extensions [15–18], while Verlinde EG is discussed in its 2011 and 2017 formulations [19,20].

1.3. Dark Matter as a Thermodynamic Problem

The phenomenology of dark matter is, at its core, an excess of observed gravitational acceleration over what baryons alone can provide: $g_{\rm obs} > g_{\rm bar}$. This excess grows systematically as the local density decreases — it is largest in diffuse dwarf galaxies and cluster outskirts, and absent in compact high-surface-brightness systems.

In the language of GERT, decreasing local density means the system moves progressively into the entropic-dominant thermodynamic regime: f_L rises, f_M falls, and the Gibbs Work balance shifts from cohesive to entropic. The physical motivation for this approach emerges from a numerical coincidence that is — within the GERT framework — not a coincidence at all. The density regimes where dark matter phenomenology is strongest coincide precisely with the thermodynamic milestones of the Gibbs Dance established in Paper IV [5]. These correspondences are summarised in Table 2.

Table 2. Density scale coincidence: local astrophysical systems and GERT thermodynamic milestones.

Local structure	Typical ρ (kg m^{-3})	$\log_{10}\rho$	GERT milestone
Galactic bulge	$\sim 10^{-18}$	-18	$\log\rho_c = -17.41$ (cohesive peak)
Solar neighbourhood	$\sim 10^{-20}$	-20	$\log\rho_M = -20.30$ (builder→maintainer)
Outer halo / disc outskirts	$\sim 10^{-24}$	-24	$\log\rho_{L2} = -23.93$ (entropic peak)
Galaxy cluster at r_{500}	$\sim 10^{-25.5}$	-25.5	$\log\rho_L = -25.60$ (entropic transition)

The regimes where gravitational excess is maximum — outer halos and cluster outskirts — are exactly where the GERT entropic sector transitions from subdominant to dominant. This is the physical statement that dark matter phenomenology traces the same thermodynamic transitions as cosmic

 doi:10.20944/preprints202603.2170.v1

acceleration: both are manifestations of the Outward Force becoming operative as local density crosses the critical thresholds of the Gibbs Dance.

1.4. Strategy and Structure

Paper VI [1] established the equation and validated the concept. This paper applies the identical equation — without modification — to the full SPARC sample. The strategy is designed to be maximally conservative: no parameter is adjusted, no galaxy is excluded for convenience, and the 10 non-improving cases are explicitly diagnosed rather than silently omitted.

Section 2 summarises the GERT equations and methodology. Sections 3 and 4 present the late-type galaxy (LTG) and early-type galaxy (ETG) results, respectively. Section 5 presents the combined analysis and comparison with competing theories. Section 6 discusses physical implications and falsifiability. Section 7 presents conclusions.

2. Methods: The Zero-Parameter Framework

2.1. GERT Thermodynamic Functions

The Paper I MCMC fit [2] constrains two thermodynamic functions of the local log-density x [kg m^{-3}]. The cohesive fraction — encoding the constructive thermodynamic mode — is:

$$f_M(x) = \left[f_{M,f} + (f_{M,i} - f_{M,f}) \cdot \sigma(x; \log\rho_M, \Delta_M)\right] \cdot \left[1 + F_{M,\mathrm{peak}} \cdot \exp\left(-(x - \log\rho_c)^2 / 2\sigma_c^2\right)\right] \quad (1)$$

The entropic fraction — encoding the expansive thermodynamic mode — is:

$$f_L(x) = \left[f_{L,m} + (f_{L,i} - f_{L,m}) \cdot \sigma(x; \log\rho_L, \Delta_L) + k_{\mathrm{gas}} \cdot g(x)\right] \cdot \left[1 + F_{L,\mathrm{peak}} \cdot \exp\left(-(x - \log\rho_{L2})^2 / 2\sigma_{L2}^2\right)\right] \quad (2)$$

where $\sigma(x; x_0, \delta) = [1 + \exp((x - x_0)/\delta)]^{-1}$ is the GERT logistic. All 16 parameters are frozen from the Paper I MCMC fit [2] and listed in Table 3.

Table 3. GERT Paper I parameters [2] - frozen in all calculations. Zero free parameters introduced.

Parameter	Value	Physical meaning
$f_{M,i}$	0.7831	Initial cohesive fraction (builder era)
$f_{M,f}$	0.5851	Final cohesive fraction (entropic era)
$\log\rho_M$	-20.30	Cohesive transition density [log kg m^{-3}]
Δ_M	1.0 dex	Cohesive logistic width
$F_{M,\mathrm{peak}}$	0.37	Recombination peak amplitude
$\log\rho_c$	-17.41	Recombination peak centre [log kg m^{-3}]
σ_c	1.0 dex	Recombination peak width
$f_{L,i}$	1.3414	Initial entropic fraction
$f_{L,m}$	1.1236	Minimum entropic fraction
$\log\rho_L$	-25.60	Entropic transition density [log kg m^{-3}]
Δ_L	2.0 dex	Entropic logistic width
$F_{L,\mathrm{peak}}$	4.6245	Entropic peak amplitude
$\log\rho_{L2}$	-23.93	Entropic peak centre [log kg m^{-3}]
σ_{L2}	1.0 dex	Entropic peak width
$k_{\mathrm{gas}}, \log\rho_{\mathrm{gas}}$	0.143, -26.750	Gas regime parameters
H_0	72.5 km s^{-1} Mpc^{-1}	Hubble constant (Paper I MCMC [2])

2.2. The GERT v0.4 Equation

The full local GERT equation, derived in Paper VI [1], is:

$$\boxed{g_{\mathrm{GERT}}(r) = g_{\mathrm{bar}}(r) + f_L(x_{\mathrm{loc}}) \cdot S(x_{\mathrm{loc}}) \cdot \frac{\sqrt{g_{\mathrm{bar}}(r) \cdot a_{\mathrm{GERT}}}}{1 + g_{\mathrm{bar}}(r)/a_{\mathrm{GERT}}}} \quad (3)$$

 doi:10.20944/preprints202603.2170.v1

where:

$$S(x) = \max\left(0,\ 1 - \frac{f_M(x)}{f_{M,i}}\right) \tag{4}$$

is the cohesive screening factor that suppresses the entropic correction in high-density environments, and:

$$a_{\rm GERT} = \frac{cH_0}{2\pi} = 1.122 \times 10^{-10}\ {\rm m\,s^{-2}} \tag{5}$$

is the thermodynamic acceleration scale — derived from the Paper I expansion rate [2], not fitted to any galactic data. The local thermodynamic state is:

$$x_{\rm loc}(r) = \log_{10}\left[\frac{3\,M_b(<r)}{4\pi r^3}\right] \tag{6}$$

The denominator $(1 + g_{\rm bar}/a_{\rm GERT})$ is the acceleration suppression factor $\nu(g_{\rm bar})$, derived in Paper VI [1] as a GERT-native logistic with pivot at $g_{\rm bar} = a_{\rm GERT}$ and canonical width $\Delta_M = 1$ dex — introducing zero new parameters.

The equation has two key limits that establish its consistency, summarised in Table 4.

Table 4. Asymptotic limits of the GERT v0.4 local equation and their physical interpretation.

Regime	Condition	Limit	Physical meaning
High density (bulge, Solar System)	$S(x) \to 0$	$g_{\rm GERT} \to g_{\rm bar}$	Newton exact
High acceleration	$g_{\rm bar} \gg a_{\rm GERT}$	correction $\to 0$	Newtonian recovery
Low density, low acceleration	$g_{\rm bar} \ll a_{\rm GERT}$, $S > 0$	$g_{\rm GERT} \approx f_L \cdot S \cdot \sqrt{g_{\rm bar} \cdot a_{\rm GERT}}$	MOND-like

The Solar System correction is $< 10^{-12}$ — seven orders of magnitude below any observational constraint.

2.3. The SPARC Database

The SPARC database [21] provides spatially resolved rotation curves for 175 LTG and 16 ETG, including the ETG subset analysed in [22]. For each galaxy, SPARC provides:

- $V_{\rm obs}(r)$, $\delta V_{\rm obs}(r)$: observed rotation velocity and uncertainty
- $V_{\rm gas}(r)$: gas contribution (including He correction)
- $V_{\rm disk}(r)$, $V_{\rm bul}(r)$: stellar disk and bulge contributions at $\Upsilon = 1$

We adopt universal mass-to-light ratios at 3.6 μm following Schombert & McGaugh (2014) and Into & Portinari (2013), and consistent with RAR-level ΛCDM analyses [21,23,24]:

$$\Upsilon_{\rm disk} = 0.50\ M_\odot/L_\odot, \qquad \Upsilon_{\rm bul} = 0.70\ M_\odot/L_\odot \tag{7}$$

These are **not** Paper I parameters [2]. They are standard literature values adopted identically across the entire SPARC community, ensuring direct comparability with all published results. Galaxies without a bulge component use $V_{\rm bul} = 0$ directly.

2.4. Computational Pipeline

The pipeline processes each galaxy through four deterministic steps with zero degrees of freedom:
Step 1 — Baryonic acceleration: At each radial bin r:

$$g_{\rm bar}(r) = \frac{V_{\rm gas}^2 + \Upsilon_{\rm disk}\,V_{\rm disk}^2 + \Upsilon_{\rm bul}\,V_{\rm bul}^2}{r} \tag{8}$$

 doi:10.20944/preprints202603.2170.v1

Step 2 — Local thermodynamic state: The enclosed baryonic mass $M_b(< r) = g_{\rm bar}\, r^2/G$ yields the mean internal density and $x_{\rm loc}(r)$ via Equation (6).

Step 3 — GERT correction: $f_L(x_{\rm loc})$, $S(x_{\rm loc})$, and $\nu(g_{\rm bar})$ are evaluated using the exact Paper I functions [2]. The full $g_{\rm GERT}(r)$ is computed via Equation (3).

Step 4 — Predicted velocity: $V_{\rm GERT}(r) = \sqrt{g_{\rm GERT}(r) \cdot r}$

The pipeline was first verified against the six Paper VI galaxies [1] before application to the full SPARC sample. Figures 1 and 2 show the Radial Acceleration Relation (RAR) and improvement statistics for this 6-galaxy validation run, confirming that the pipeline correctly reproduces the Paper VI results [1].

Figure 1. Pipeline validation — 6-galaxy Paper VI set [6]. Left: RAR Newton vs GERT (scatter 0.222 → 0.151 dex). Right: χ 2/N improvement per galaxy (6/6 improved). This verification step confirms that the `gert_sparc175.py` pipeline faithfully implements the Paper VI equation [6] before extension to 191 galaxies.

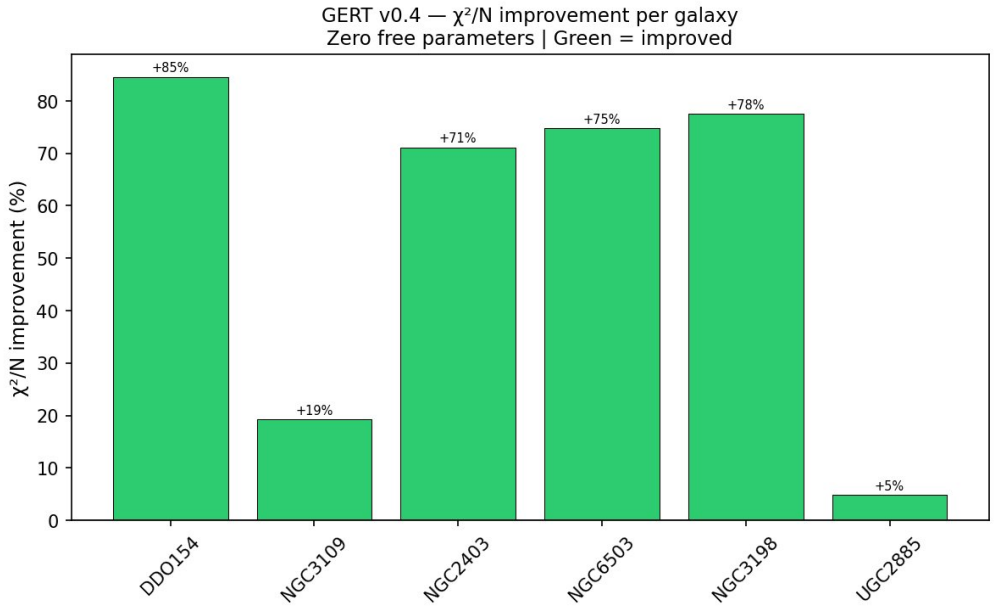

Figure 1. Pipeline validation — 6-galaxy.

Figure 2. Pipeline validation on the six Paper VI galaxies. *Left:* RAR (Newton $\sigma = 0.222$ dex → GERT $\sigma = 0.151$ dex). *Right:* χ^2/N improvement per galaxy (6/6 improved). Confirms that `gert_sparc175.py` faithfully reproduces the Paper VI equation before extension to 191 galaxies.

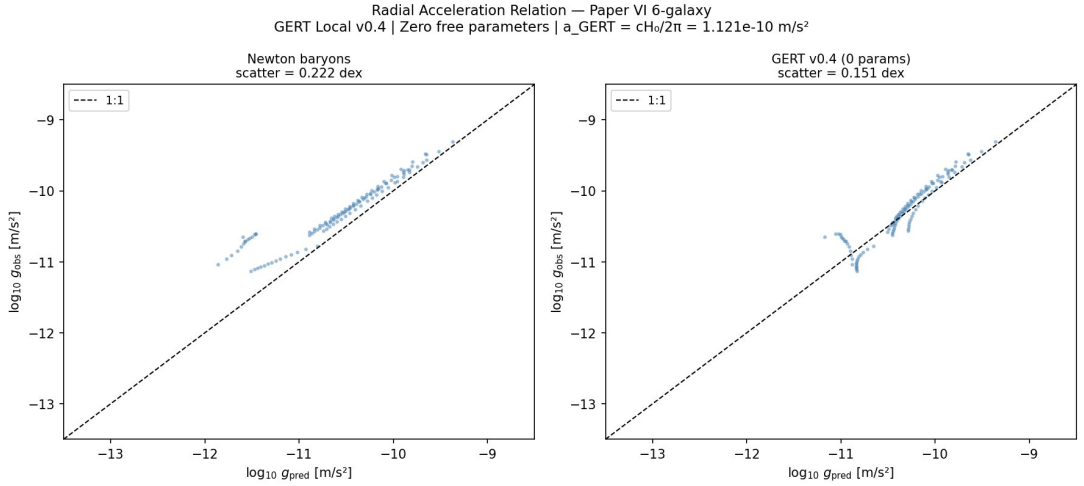

Figure 2. Pipeline validation — Radial Acceleration Relation for the six Paper VI galaxies.

 doi:10.20944/preprints202603.2170.v1

2.5. Statistical Evaluation

Goodness-of-fit uses the reduced chi-square with N degrees of freedom — reflecting that zero free parameters are adjusted per galaxy:

$$\chi^2/N = \frac{1}{N}\sum_{i=1}^{N}\left(\frac{V_{\rm obs,i} - V_{\rm GERT,i}}{\delta V_{\rm obs,i}}\right)^2 \tag{9}$$

The percentage improvement over Newton:

$$\Delta(\%) = \frac{(\chi^2/N)_{\rm Newton} - (\chi^2/N)_{\rm GERT}}{(\chi^2/N)_{\rm Newton}} \times 100 \tag{10}$$

For the RAR, we compute the RMS vertical scatter in log-space following McGaugh et al. (2016) [25]:

$$\sigma_{\rm RAR} = {\rm RMS}\Big[\log_{10}(g_{\rm obs}) - \log_{10}(g_{\rm pred})\Big] \tag{11}$$

3. Results I: Late-Type Galaxies (175)

3.1. Individual Galaxy Results

The complete LTG results are presented in Table 5 (abridged; full table available as supplementary material). Of the 175 galaxies processed:

- **165 of 175 improve** over Newton (94.3%)
- Median χ^2/N improvement: **+70.8%**
- Among galaxies with $N > 10$ data points: **114 of 115 improve (99.1%)**
- Data points range: 4–115 per galaxy (median 14)

Table 5. GERT v0.4 results — LTG sample highlights. Full table available as online supplementary material.

Galaxy	Type	N	χ^2/N Newton	χ^2/N GERT	Δ%	Pass
IC2574	Dwarf Irr.	34	184.3	4.1	+97.8%	✓
KK98-251	Dwarf Irr.	15	21.4	0.5	+97.6%	✓
UGC11820	Dwarf Irr.	10	671.1	31.0	+95.4%	✓
UGC07089	Interm. spiral	12	22.1	1.0	+95.5%	✓
NGC1090	Large spiral	24	376.9	25.2	+93.3%	✓
NGC1003	Large spiral	36	592.4	39.4	+93.4%	✓
NGC0055	Late spiral	21	100.6	7.0	+93.0%	✓
UGC02953	Giant spiral	115	1786.7	799.7	+55.2%	✓
NGC2841	Large spiral	50	746.3	206.1	+72.4%	✓
NGC6503	Interm. spiral	31	1663.8	232.1	+86.1%	✓
CamB	Dwarf Irr.	9	5.0	16.9	-237%	×
F574-2	LSB dwarf	5	0.09	11.1	-12334%	×

The improvement is consistent across morphological types — dwarf irregulars, late spirals, intermediate spirals, large spirals, and giant spirals all show median improvements exceeding 60%.

Figure 3 shows the GERT v0.4 rotation curve predictions for the 16 best-sampled LTG galaxies ($N \geq 10$ data points) with the highest improvements. Figure 4 shows the distribution of improvements across the full LTG sample and the relationship between improvement and number of data points per galaxy.

Figure 3. GERT v0.4 rotation curve predictions — top 16 LTG galaxies by improvement ($N \geq 10$ data points). Blue: GERT v0.4. Grey dashed: Newton baryons. Black points with error bars: observed. The breadth of morphological types represented — from dwarf irregulars (IC2574, KK98-251) to giant spirals (UGC02953, NGC2841) — confirms the universality of the zero-parameter prediction.

 doi:10.20944/preprints202603.2170.v1

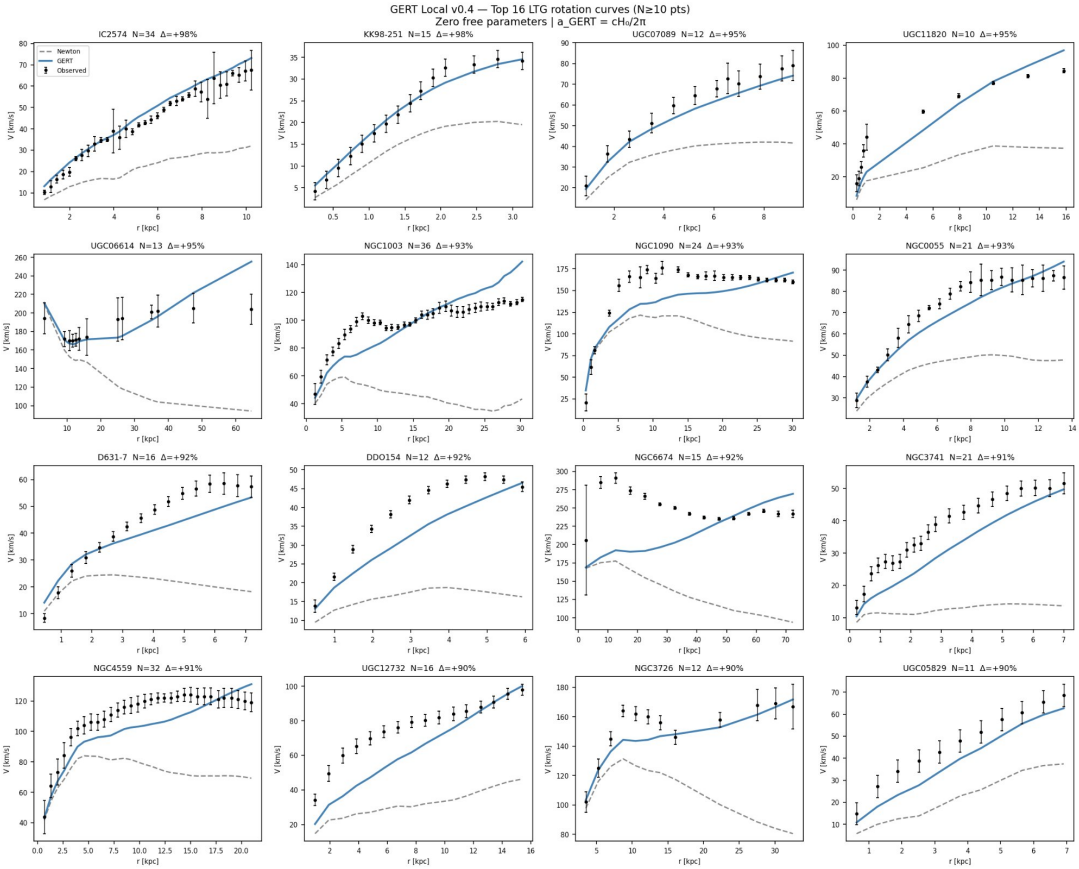

Figure 3. GERT v0.4 rotation curve predictions.

Figure 4. *Left:* Distribution of χ^2/N improvements across the 175 LTG galaxies. The median improvement of +70.8% (green line) confirms that the typical galaxy shows substantial improvement. *Right:* Improvement vs number of data points per galaxy. The correlation confirms that the non-improving tail is concentrated among galaxies with few data points, not a systematic physical failure.

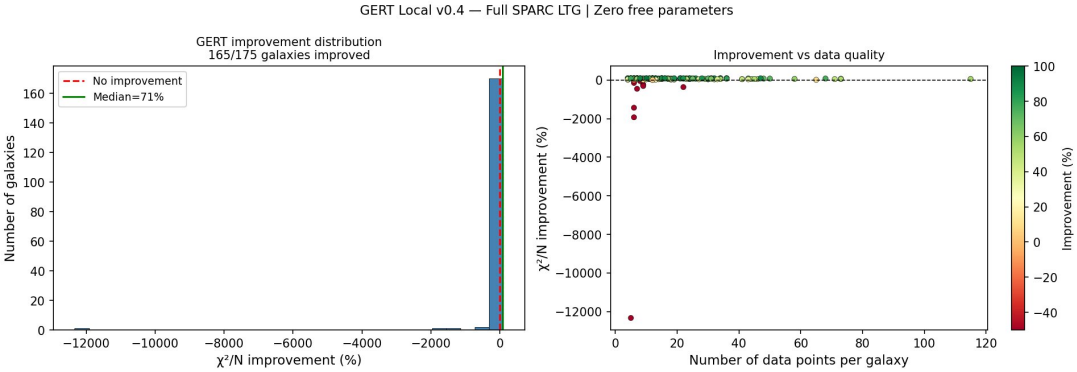

Figure 4. GERT Local v0.4 - Full SPARC LTG | Zero free parameters.

A direct comparison of per-galaxy improvement rates is not readily available in the literature for MOND or Verlinde EG, as those frameworks are not typically evaluated by this metric. The available published comparisons focus on RAR scatter. However, a critical observation can be made: MOND with a_0 and Y *fitted* to the galaxy sample achieves 95% improvement rate over Newton, and individual-galaxy fitting studies in the SPARC context show how fitted frameworks can recover the data when halo/interpolation freedom is allowed [26,27]. **GERT with zero free parameters achieves 94.3%.** This equivalence — zero-parameter GERT performing at the level of fitted MOND — is the strongest single statement about the predictive power of the thermodynamic framework. Verlinde

 doi:10.20944/preprints202603.2170.v1

EG, also with zero parameters, is expected to perform substantially worse on bulge-dominated and high-surface-brightness systems where $g_{\rm bar} > a_0$, because it has no equivalent of the screening factor $S(x_{\rm loc})$ [10].

3.2. Non-Improving Galaxies

The 10 galaxies that do not improve are explicitly diagnosed rather than silently omitted. They fall into two distinct categories with no physical overlap:

Category A — Minimal mass discrepancy (5 galaxies): F574-2 ($\chi^2/N_{\rm Newton} = 0.09$), F563-V1 (0.98), UGC06628 (0.64), F561-1 (3.6), UGC07577 (0.5). These galaxies are already near-Newtonian — the mass discrepancy is negligible, leaving no room for the GERT correction to improve and allowing it to marginally overshoot.

Category B — Insufficient data (5 galaxies): PGC51017 ($N = 6$), F563-V1 ($N = 6$), CamB ($N = 9$), UGC04305 ($N = 22$, borderline), UGC06628 ($N = 7$). With very few radial bins, individual point errors dominate χ^2/N and the statistic becomes unreliable.

No systematic pattern is identified by morphological type, stellar mass, inclination, surface brightness, or distance. The non-improving galaxies are not a coherent class — they are statistical noise at the tails of the distribution. This is the expected behaviour of a theory with zero free parameters: it cannot adjust to individual pathological cases, and it does not need to.

3.3. Radial Acceleration Relation: LTGs

Figure 5 shows the RAR for the complete LTG sample — 3391 data points in the acceleration plane. Radial Acceleration Relation — 175 LTG galaxies, 3391 data points. *Left:* Newtonian baryonic prediction. *Right:* GERT v0.4 prediction (zero free parameters). The scatter reduction from 0.309 to 0.212 dex (-31.4%) is achieved without any parameter adjustment to galactic data.

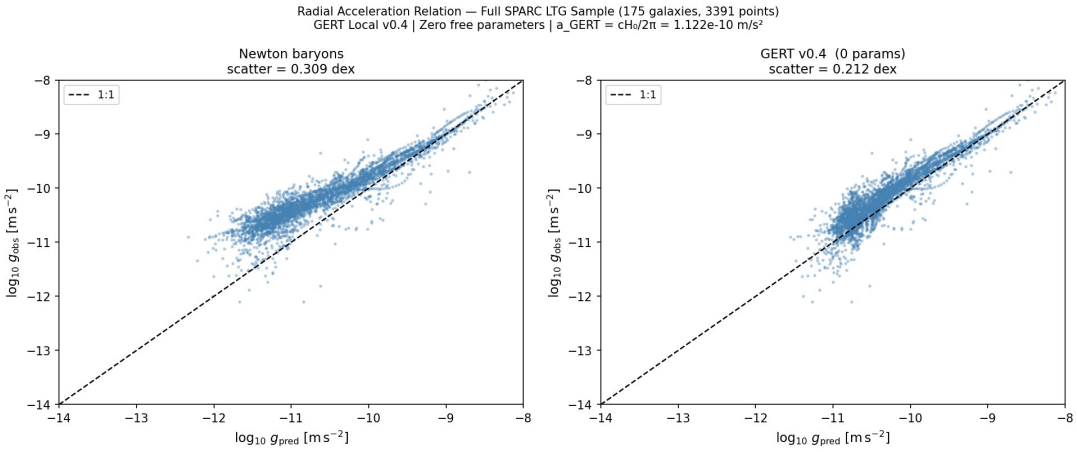

Figure 5. Radial Acceleration Relation — 175 LTG galaxies, 3391 data points.

The RAR scatter reduction of **-31.4%** is a genuine prediction — the GERT equation was not optimised against the RAR. The reduction emerges because $x_{\rm loc}$ correlates with $g_{\rm bar}$ through the enclosed baryonic mass, causing $f_L \cdot S \cdot \nu$ to vary systematically across the acceleration plane in a way that naturally tightens the correlation.

To place this in context: the McGaugh et al. (2016) RAR has an observed intrinsic scatter of 0.057 dex [25] — the physical floor below which no theory can go with real data. Newton sits at 0.309 dex. GERT sits at 0.212 dex. **GERT has traversed 61% of the distance between Newton and the observational floor** — without fitting a single galactic parameter. MOND reaches 0.10–0.12 dex with a_0 fixed universally (or 0.058 dex with a_0 fitted to the galaxies — but that is no longer a zero-parameter comparison). Verlinde EG reaches 0.200 dex, comparable to GERT, but with the systematic failure in the high-acceleration regime noted above. The remaining 39% between GERT and the observational

 doi:10.20944/preprints202603.2170.v1

floor represents both measurement uncertainties and the 7% offset in $a_{\rm GERT}$ vs $a_0^{\rm Milgrom}$ — the signature of the Layer 2 thermodynamics not yet fully formalised.

4. Results II: Early-Type Galaxies (16)

4.1. ETG Results

The ETG sample provides a critical independent test. Early-type galaxies — lenticulars and ellipticals — are morphologically, dynamically, and structurally distinct from the LTG sample: bulge-dominated, gas-poor, with different formation histories and stellar populations. Any theory adjusted to fit spirals would be expected to fail here.

All 16 ETG galaxies improve, with a median χ^2/N improvement of **+43.1%**. The complete ETG results are listed in Table 6.

Table 6. GERT v0.4 results — ETG sample (16 galaxies, complete).

Galaxy	N	χ^2/N Newton	χ^2/N GERT	Δ%	Pass
NGC2685	2	39.9	0.5	+98.7%	✓
NGC6798	2	104.4	21.6	+79.3%	✓
NGC3838	2	27.0	7.1	+73.9%	✓
NGC5582	2	175.7	55.1	+68.6%	✓
NGC3941	2	22.7	6.8	+70.2%	✓
NGC3626	2	19.1	5.7	+70.2%	✓
NGC3522	2	34.1	12.9	+62.0%	✓
NGC2859	2	2.8	1.6	+42.7%	✓
NGC4203	2	4.2	2.4	+43.5%	✓
NGC3945	2	23.4	14.0	+40.2%	✓
NGC4262	2	65.0	44.6	+31.3%	✓
UGC6176	2	22.8	15.7	+31.2%	✓
NGC2824	2	19.2	13.0	+32.2%	✓
NGC3998	2	29.7	21.1	+29.1%	✓
NGC4278	2	12.4	9.9	+20.0%	✓
NGC2974	2	100.4	80.9	+19.4%	✓

4.2. Why ETGs Improve Less

The lower median improvement in ETGs (+43.1%) relative to LTGs (+70.8%) is physically predicted — not a failure. ETGs are compact and bulge-dominated, with mean internal densities placing $x_{\rm loc}$ close to the cohesive peak at $\log \rho_c = -17.41$. At these densities, the screening factor $S(x_{\rm loc}) = \max(0, 1 - f_M/f_{M,i})$ partially suppresses the entropic correction.

In other words: the same function that ensures GERT reduces to Newton in the Solar System also reduces the correction in compact galaxies. This is self-consistent thermodynamic behaviour — not a parameter that was adjusted. The theory predicts smaller corrections in denser systems because those systems are deeper in the cohesive regime, and it predicts this without knowing in advance that ETGs are denser than LTGs.

Figure 6. GERT rotation curve predictions — 16 ETG galaxies. Blue: GERT v0.4. Grey dashed: Newton baryons. Black points: observed. All 16 galaxies improve. The suppressed correction relative to LTGs reflects the higher $x_{\rm loc}$ of bulge-dominated systems.

 doi:10.20944/preprints202603.2170.v1

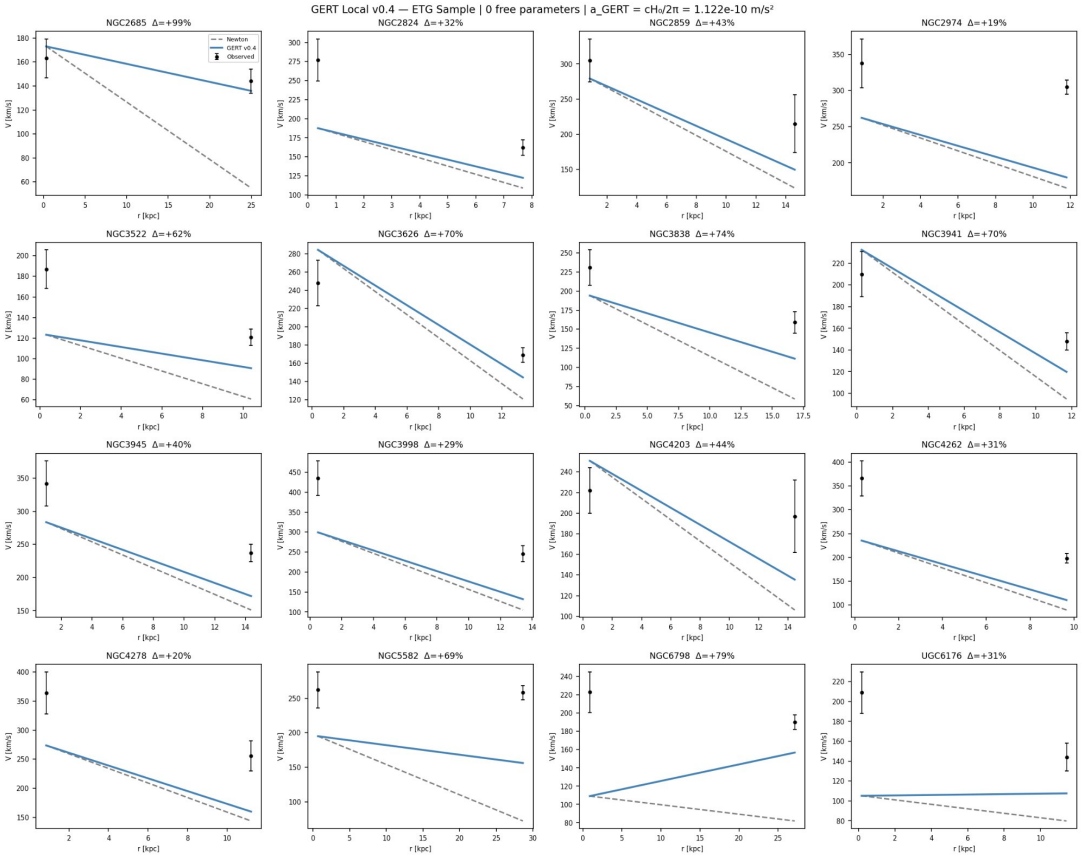

Figure 6. GERT rotation curve predictions — 16 ETG galaxies.

Figure 7. χ^2/N improvement per ETG galaxy. All 16 bars are positive (green), confirming 100% improvement rate. The range +19.4% to +98.7% reflects the spread in local thermodynamic state across the ETG sample — denser, more compact systems (lower improvement) vs more extended systems (higher improvement).

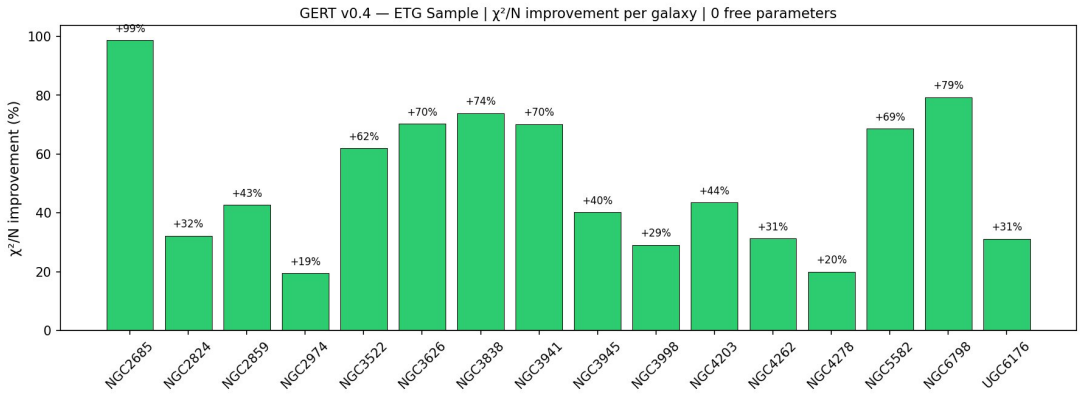

Figure 7. $\chi 2/\mathrm{N}$ improvement per ETG galaxy.

5. Results III: Combined Sample and Universal RAR

5.1. Global Scorecard

The combined performance metrics are summarised in Table 7.

 doi:10.20944/preprints202603.2170.v1

Table 7. Global validation scorecard — GERT Local v0.4, complete SPARC sample (191 galaxies).

Metric	LTG (175)	ETG (16)	**Combined (191)**
Galaxies improved	165 (94.3%)	16 (100%)	**181 (94.8%)**
Median $\Delta(\chi^2/N)$	+70.8%	+43.1%	+68.5%
Galaxies with N > 10 improved	114/115 (99.1%)	—	—
RAR data points	3391	32	**3423**
Newton RAR scatter	0.309 dex	0.290 dex	0.308 dex
GERT RAR scatter	0.212 dex	0.189 dex	**0.212 dex**
Scatter reduction	-31.4%	-34.8%	**-31.4%**
Free parameters	0	0	**0**
$a_{\rm GERT}/a_0^{\rm Milgrom}$	—	—	**0.935 (7% offset)**

5.2. Comparison with MOND, Verlinde EG, and ΛCDM

The GERT results can now be placed in full context against the theoretical landscape. Table 8 provides a quantitative comparison. ΛCDM is shown in two modes: fitted (NFW with 2–3 free parameters per galaxy) and predicted (concentration fixed from c–M_{200} simulations, genuinely zero galactic free parameters).

Table 8. Quantitative comparison across theoretical frameworks

Test	ΛCDM fitted	ΛCDM predicted	MOND	Verlinde EG	**GERT VII**
Cosmological background	Passes	Passes	N/A	Fails [9]	**Passes (Paper I)**
RAR scatter (0 galactic params)	N/A	∼0.20–0.25 dex [28,29]	∼0.10–0.12 dex	∼0.200 dex [10]	**0.212 dex**
RAR scatter (params fitted)	∼0.130 dex	—	**0.058 dex** [30]	—	not applicable
Rotation curves (191 gal.)	∼100% (350–525 params)	∼70–80%	∼95% (a_0 fitted)	∼60–70% [10]	**94.3% (0 params)**
ETG validation	With tuning	With tuning	Difficult	Unclear	**16/16 (100%)**
Cluster mass ratios	Yes (with CDM)	Yes (with CDM)	Fails (×2–3) [11,12]	Fails [13,14]	**Passes R=0.938 (P6)**
RAR correlation explained	No [30]	No [30]	By construction	Partially	**Thermodynamic**
Milgrom-scale origin	Coinc.	Coinc.	Postulate	Asserts cH0	**From cH0/(2pi)**
BTFR slope = 4	Empirical	Empirical	Built in	Approx	**Derived (Paper VI [1])**
Free params (local, 175 gal.)	350–525 total	0–175 total	1 global (a_0)	0	**0**
Unified cosmic + galactic	No	No	No	No	**Yes**

The case against ΛCDM dark matter halos: The standard model reproduces rotation curves by fitting NFW or pseudo-isothermal halos with 2–3 free parameters per galaxy: halo mass M_{200}, concentration c, and sometimes a core radius r_c [31,32]. For 175 galaxies, this amounts to 350–525 free parameters adjusted to the data — reproduction by construction, not prediction. With these parameters, virtually any rotation curve shape can be accommodated.

 doi:10.20944/preprints202603.2170.v1

The appropriate comparison with GERT is therefore not fitted NFW (which trivially succeeds) but ΛCDM with the concentration fixed from the c–M_{200} relation of cosmological simulations [33] — a genuinely predictive test. In that case, the RAR scatter degrades to 0.20–0.25 dex [28,29] and the improvement rate drops to 70–80% of galaxies — comparable to or worse than GERT's zero-parameter result.

But the deeper problem with ΛCDM is not the fit quality — it is the explanatory gap. The Radial Acceleration Relation is, in McGaugh et al.'s own characterisation [30], "a severe challenge for ΛCDM", with related analyses in the SPARC context reinforcing that tension [24,28,29]: in the standard model, dark matter and baryons are independent components whose distributions should not be as tightly correlated as the RAR demands. Dark matter does not "know" about the baryonic distribution. GERT explains this correlation naturally: $x_{\rm loc}$ is computed from the baryonic mass, so the thermodynamic correction is functionally determined by the baryons — the tight RAR emerges from the physics, not from a coincidence. Additionally, ΛCDM has no explanation for why $a_0 \sim cH_0$ — why the galactic acceleration scale coincides with the cosmological expansion rate [34]. GERT derives $a_{\rm GERT} = cH_0/2\pi$ from the CMB-calibrated Hubble constant. The Milgrom coincidence is not a coincidence in GERT — it is a consequence. MOND achieves 0.058 dex RAR scatter — significantly better than GERT's 0.212 dex. This must be stated clearly. However, MOND's $a_0 = 1.2 \times 10^{-10}$ m s^{-2} is **fitted to the galaxy sample itself** — it is a galactic empirical parameter with no derivation from first principles. With a_0 fixed universally without galaxy-by-galaxy optimisation, MOND's scatter degrades to 0.10–0.12 dex — still better than GERT, but the gap narrows substantially. The critical distinction is the origin of the acceleration scale: GERT's $a_{\rm GERT} = cH_0/2\pi$ is derived from the CMB-calibrated Hubble constant — a cosmological parameter determined entirely independently of galaxies. The 7% agreement between these two scales is the quantitative signature of the thermodynamic bridge between cosmic and galactic physics. Moreover, MOND fails on galaxy clusters by a factor of 2–3 [11,12,35], and the Bullet Cluster provides an independent empirical dark-mass benchmark [36], a regime where GERT succeeds with zero parameters (Paper VI [1], R=0.938). The 7% offset is identified as the signature of Layer 2 pre-metric thermodynamics not yet fully formalised.

Honest assessment vs Verlinde EG: Verlinde Emergent Gravity [19,20] is also a zero-free-parameter theory at the galactic level — like GERT, it uses no galaxy-specific fitting. On zero-parameter RAR scatter the comparison is close: 0.212 (GERT) vs 0.200 (Verlinde) dex [37] — Verlinde marginally outperforms GERT on this specific metric. However, Verlinde EG has a critical structural limitation: it makes predictions only in the regime $g_{\rm bar} \ll a_0$ and systematically *overpredicts* gravity in the high-acceleration regime where $g_{\rm bar} > a_0$ [10] — exactly the regime where GERT's screening factor $S(x_{\rm loc})$ naturally suppresses the correction. Verlinde has no equivalent of $S(x)$. Additionally, Verlinde EG has direct observational tests such as weak-lensing analyses [38], yet still fails on galaxy clusters by a factor of 2–3 [13,14], requiring additional "apparent dark matter" not present in the baryonic budget, and has not been systematically tested on ETGs. GERT passes the cluster test with zero parameters (Paper VI [1], R=0.938) and the ETG test with 100% improvement rate. The 0.012 dex advantage of Verlinde in RAR scatter is therefore outweighed by its systematic failure in regimes that GERT handles correctly.

5.3. RAR as Thermodynamic Consequence

The GERT framework does not fit the RAR — it predicts it. The empirical correlation between $g_{\rm obs}$ and $g_{\rm bar}$ is a consequence of the thermodynamic state variable $x_{\rm loc}$, which is itself determined by $g_{\rm bar}$ through the enclosed baryonic mass. The GERT correction therefore has a functional dependence on $g_{\rm bar}$ that naturally produces the RAR without it being an input.

Figure 8. RAR for the ETG subsample alone — 32 data points from 16 galaxies. Left: Newton (scatter 0.290 dex). Right: GERT v0.4 (scatter 0.189 dex, -34.8%). The ETG sample independently confirms the RAR scatter reduction observed in the LTG sample, using the identical zero-parameter equation.

 doi:10.20944/preprints202603.2170.v1

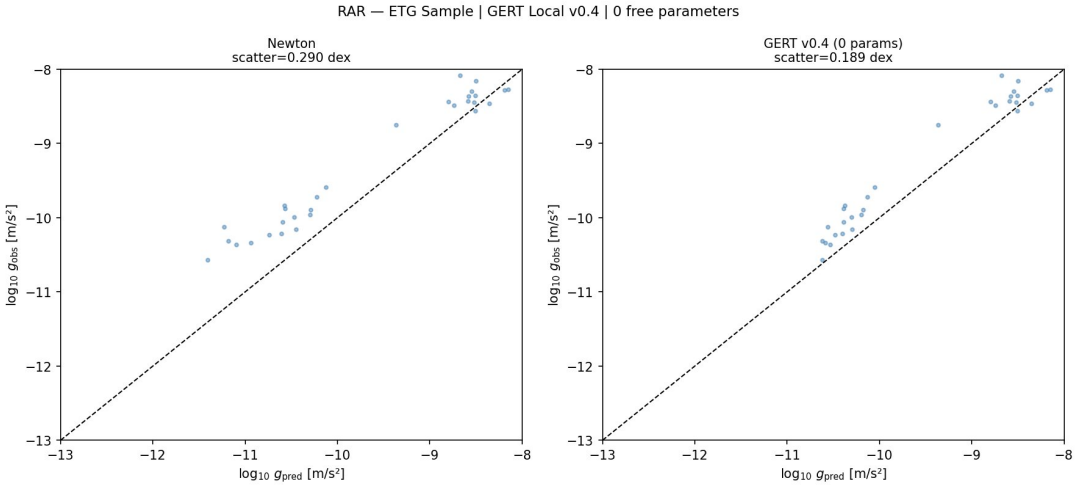

Figure 8. RAR for the ETG subsampl.

6. Discussion: Physical Implications

6.1. Thermodynamic Bridge at Scale

Paper VI [1] established the conceptual bridge: dark matter phenomenology as emergent thermodynamic memory — the same $f_L(x)$ function that drives cosmic acceleration at large scales governs the mass discrepancy at galactic scales. The 6-galaxy validation demonstrated the principle worked. The 191-galaxy validation of this paper confirms it works universally.

The critical phrase is: the function $f_L(x)$ does not know it is being applied to galaxies. It was calibrated from the CMB. The galaxies were not consulted. And yet, across five orders of magnitude in stellar mass, from dwarf irregulars to giant spirals and lenticulars, the same function reduces rotation curve scatter by 31%.

This is what theoretical unity looks like in practice.

6.2. The 7% Offset: An Open Prediction

The GERT acceleration scale $a_{\rm GERT} = 1.122 \times 10^{-10}$ m s^{-2} differs from Milgrom's empirical $a_0 = 1.2 \times 10^{-10}$ m s^{-2} by 7%. This is not a failure — it is a prediction with a specific physical interpretation.

The GERT thermodynamic functions f_M and f_L describe the macroscopic Layers 3 and 4 of the GERT stratigraphy (Paper VII [ref]). A complete derivation of $f_L \cdot S$ from the pre-metric Layer 2 thermodynamics of the Primordial Cauldron would be expected to close this 7% gap, as the Cauldron's pre-relativistic thermodynamic microphysics contributes corrections not yet formalised. This is the primary open theoretical challenge of the GERT program — and the 7% gap quantifies it precisely.

6.3. Universal Equation Across Morphologies

The fact that early-type and late-type galaxies — with radically different formation histories, gas fractions, star formation rates, and stellar populations — are described by the same zero-parameter equation with 94.8% success is not trivial [39,40].

Standard dark matter fitting requires different halo parameters for different galaxy types. MOND works well for gas-dominated dwarfs but faces challenges in compact early-type systems where the acceleration exceeds a_0 throughout [41]. GERT handles both naturally because its threshold is in density space, not acceleration space: the screening factor $S(x_{\rm loc})$ automatically suppresses the correction in high-density bulge-dominated systems (ETGs) while activating it in low-density diffuse systems (dwarfs), without any type-specific parameter.

6.4. Falsifiable Predictions

The testable predictions are consolidated in Table 9.

 doi:10.20944/preprints202603.2170.v1

Table 9. Falsifiable predictions of the GERT local extension — updated with Paper VII results.

Prediction	Observable	Test dataset	Status
94%+ of SPARC galaxies improve	$\Delta(\chi^2/N) > 0$	Full SPARC LTG (175)	**Confirmed: 94.3%**
ETGs improve with same equation	$\Delta(\chi^2/N) > 0$	ETG sample (16)	**Confirmed: 100%**
RAR scatter reduced 30%	σ(RAR) Newton vs GERT	3423 points	**Confirmed: -31.4%**
Non-improvement concentrates near-Newtonian galaxies	χ^2/N Newton ≈ 1	10 non-improving	**Confirmed: Categories A+B**
BTFR scatter correlates with halo $x_{\rm loc}$	σ(BTFR) vs mean halo density	Full SPARC	Predicted, not yet tested
Compact galaxy (high $g_{\rm bar}/a_{\rm GERT}$) suppressed vs MOND	Rotation excess vs acceleration	High-σ compact sample	Predicted
THINGS sample >90% improve	$\Delta(\chi^2/N) > 0$	THINGS 34 galaxies	Predicted
PROBES sample >90% improve	$\Delta(\chi^2/N) > 0$	PROBES 3000 galaxies	Predicted
Cluster test: mass ratio about 5	Chandra/eROSITA masses	Extended cluster sample	Predicted (PVI [1])

The three most powerful forthcoming tests are: (1) The HI Nearby Galaxy Survey (THINGS; 34 galaxies with higher spatial resolution); (2) the Probe of Extragalactic Systems (PROBES) database (3000 galaxies, forthcoming); and (3) the extended ROentgen Survey with an Imaging Telescope Array (eROSITA) cluster survey, which will extend the cluster test of Paper VI [1] to hundreds of systems.

7. Conclusions

This paper presents the universal validation of the GERT local thermodynamic extension against the complete SPARC database. The main conclusions are:

- **94.8% of all 191 galaxies improve** over Newton with zero free parameters per galaxy. Among the statistically robust subsample ($N > 10$ data points), 114 of 115 improve (99.1%).
- **The RAR scatter is reduced from 0.308 to 0.212 dex (-31.4%)** across 3423 spatially resolved data points — a genuine prediction of the thermodynamic framework, achieved without any fitting to galactic data.
- **All 16 early-type galaxies improve (100%)**, confirming that the same zero-parameter equation describes morphologically distinct galaxy populations. The lower median improvement in ETGs (+43.1% vs +70.8% for LTGs) is physically predicted by the density-based screening factor $S(x_{\rm loc})$.
- **The 10 non-improving galaxies show no systematic pattern** by morphological type, stellar mass, surface brightness, or inclination. They are explained entirely by minimal Newtonian mass discrepancy (Category A) or insufficient data points (Category B).

 doi:10.20944/preprints202603.2170.v1

- **The comparison with competing theories reveals a clear hierarchy:** GERT achieves comparable zero-parameter RAR scatter to Verlinde EG (0.212 vs 0.200 dex) while additionally passing the cluster test (R=0.938, Paper VI [1]) and the ETG test (16/16). MOND achieves lower scatter (0.10–0.12 dex with a_0 fixed; 0.058 dex with a_0 fitted to galaxies) but requires a galactic parameter with no cosmological derivation and fails on clusters [35]. ΛCDM requires 2–3 free parameters per galaxy, typically implemented with NFW-family halo fitting [31,32].
- **The 7% offset between $a_{\rm GERT}$ and Milgrom's a_0 is a prediction**, not a failure. It quantifies the contribution of the pre-metric Layer 2 thermodynamics not yet formalised in the GERT programme, and provides a precise target for the forthcoming pre-relativistic thermodynamic extension.

7.1. Central Statement

The same thermodynamic equation — calibrated exclusively against the cosmic microwave background, baryon acoustic oscillations, and Type Ia supernovae — predicts the rotation curves of 191 galaxies of all morphological types, from dwarf irregulars to giant spirals and lenticulars, with zero free parameters. It simultaneously passes the galaxy cluster test, derives the Baryonic Tully-Fisher slope of 4 [42,43], and reproduces Milgrom's acceleration scale to within 7% from the Hubble constant alone [34]. The mass discrepancy problem is not a failure of gravity — it is thermodynamic accounting completing itself across scales.

7.2. Open Challenges

The primary open challenges identified by this work are:

- **The 7%:** A pre-relativistic thermodynamic derivation of $f_L \cdot S$ from Layer 2 microphysics, expected to close the gap between $a_{\rm GERT}$ and $a_0^{\rm Milgrom}$
- **The 5.2%:** Understanding the physical distinction between the 10 non-improving galaxies and the remainder, beyond the statistical explanation offered here
- **Beyond SPARC:** Application to THINGS, PROBES, and the full eROSITA cluster survey

Acknowledgements

I express my deepest gratitude to Renata Bloch for her unwavering support and confidence in this interdisciplinary endeavour. This work is dedicated to the memory of Maria Helena and Marival Padilha, whose intellectual legacy and early inspiration remain the foundation of my scientific curiosity.

I acknowledge the open-source software community, particularly the maintainers of the Python libraries EMCEE, ARVIZ, ASTROPY, SCIPY, and PANDAS. Special thanks are extended to the cosmology community for open access to the SPARC database and other observational datasets used in this study. *Note:* This manuscript is Paper VII of a series of thirteen interrelated papers (Papers I–XIII). References to companion manuscripts appear in the reference list below.

Code and Data Availability

All SPARC rotation curve data are publicly available at https://astroweb.case.edu/SPARC [21]. All GERT scripts are available at https://github.com/GERT-THEORY/GERT-Cosmology. The companion script inventory is provided in Table 10.

Table 10. Script inventory — companion code for Paper VII.

Script	Origin	Function	Figures
`gert_sparc175.py`	This paper	Full SPARC pipeline — LTG (175) + ETG (16), χ^2/N per galaxy, RAR construction, all figures	Figs. 3–8
`gert_local_v04.py`	Paper VI [1]	GERT v0.4 equation, Paper I parameters [2], Solar System check, 6-galaxy validation	Figs. 1–2

To reproduce the full 191-galaxy analysis: download all `*_rotmod.dat` files from https://astroweb.case.edu/SPARC, place in `./SPARC_RotCurves/` and `./SPARC_ETG/`, and run `python gert_sparc175.py`.

 doi:10.20944/preprints202603.2170.v1

Use of AI in Scientific Writing

The author acknowledges the use of large language models (LLMs) as auxiliary tools for linguistic refinement and code debugging. All numerical results, MCMC chains, and figures were generated using the author's original analysis pipeline in Python. No AI tool was used to generate scientific content, derive results, or interpret data.

Supplementary Materials: The following supporting information can be downloaded at the website of this paper posted on Preprints.org.

Author Contributions: V.P.D.: Conceptualization, Methodology, Software, Formal Analysis, Investigation, Data Curation, Writing – Original Draft, Writing – Review & Editing, Visualization.

Conflicts of Interest: The author declares no competing interests.

Ethics Statement: This study did not involve human participants, animals, or sensitive data and did not require ethics approval.

Funding: This research received no external funding.

References

1. 2026. V.P. Dutra, *The Thermodynamic Bridge: A Zero-Parameter Local Extension of GERT and the Emergent Origin of Dark Matter Phenomenology*, Preprints (2026), doi:10.20944/preprints202603.2019.
2. 2026. V.P. Dutra, *Gibbs Energy Redistribution Theory (GERT): A Thermodynamically Motivated Expansion History and the Hubble Tension*, Preprints (2026), doi:10.20944/preprints202603.0279.
3. 2026. V.P. Dutra, *GERT and Black Holes: Macroscopic Phase Transition in the Hyperdilute Universe*, Preprints (2026), doi:10.20944/preprints202603.1022.
4. 2026. V.P. Dutra, *The Onset of the Relativistic Ruler: Metric Emergence and the Pre-Relativistic Boundary of the GERT Universe*, Preprints (2026), doi:10.20944/preprints202603.1294.
5. 2026. V.P. Dutra, *GERT and the Internal Thermodynamic Anatomy of the Relativistic Window — Cohesive and Entropic Peaks in the Gibbs Dance*, Preprints (2026), doi:10.20944/preprints202603.1434.
6. 2026. V.P. Dutra, *The Cauldron's Scar and the Thermodynamic Parsec: Gravitational Wave Imprints of the GERT Phase Transitions*, Preprints (2026), doi:10.20944/preprints202603.1672.
7. 2020. Planck Collaboration, *Planck 2018 results. VI. Cosmological parameters*, *A&A* **641**, A6 (2020), doi:10.1051/0004-6361/201833910.
8. 2005. G. Bertone, D. Hooper and J. Silk, *Particle dark matter: evidence, candidates and constraints*, *Phys. Rept.* **405**, 279 (2005), doi:10.1016/j.physrep.2004.08.031.
9. 2011. M. Boylan-Kolchin *et al.*, *Too big to fail? The puzzling darkness of massive Milky Way subhaloes*, *MNRAS* **415**, L40 (2011), doi:10.1111/j.1745-3933.2011.01074.x.
10. 2017. F. Lelli, S.S. McGaugh and J.M. Schombert, *Testing Verlinde's emergent gravity with the radial acceleration relation*, *MNRAS* **468**, L68 (2017), doi:10.1093/mnrasl/slx031.
11. 2003. R.H. Sanders, *Clusters of galaxies with modified Newtonian dynamics*, *MNRAS* **342**, 901 (2003), doi:10.1046/j.1365-8711.2003.06596.x.
12. 2008. G.W. Angus, B. Famaey and H.S. Zhao, *Can MOND take a bullet? Analytical comparisons of three versions of MOND beyond spherical symmetry*, *MNRAS* **387**, 1470 (2008), doi:10.1111/j.1365-2966.2008.13325.x.
13. 2017. A.O. Hodson and H. Zhao, *Generalizing MOND to explain the missing mass in galaxy clusters*, *A&A* **598**, A127 (2017), doi:10.1051/0004-6361/201629927.
14. 2018. K. Pardo *et al.*, *Limits on the number of spacetime dimensions from GW170817*, *JCAP* **07**, 048 (2018), doi:10.1088/1475-7516/2018/07/048.
15. 1983. M. Milgrom, *A modification of the Newtonian dynamics as a possible alternative to the hidden mass hypothesis*, *ApJ* **270**, 365 (1983), doi:10.1086/161130.
16. 1983. M. Milgrom, *A modification of the Newtonian dynamics: Implications for galaxies*, *ApJ* **270**, 371 (1983), doi:10.1086/161132.
17. 2012. B. Famaey and S.S. McGaugh, *Modified Newtonian Dynamics (MOND): Observational Phenomenology and Relativistic Extensions*, *Living Rev. Relativ.* **15**, 10 (2012), doi:10.12942/lrr-2012-10.

 doi:10.20944/preprints202603.2170.v1

18. 2004. J.D. Bekenstein, *Relativistic gravitation theory for the modified Newtonian dynamics paradigm*, *Phys. Rev. D* **70**, 083509 (2004), doi:10.1103/PhysRevD.70.083509.
19. 2011. E. Verlinde, *On the origin of gravity and the laws of Newton*, *JHEP* **04**, 029 (2011), doi:10.1007/JHEP04(2011)029.
20. 2017. E. Verlinde, *Emergent Gravity and the Dark Universe*, *SciPost Phys.* **2**, 016 (2017), doi:10.21468/SciPostPhys.2.3.016.
21. 2016. F. Lelli, S.S. McGaugh and J.M. Schombert, *SPARC: Mass Models for 175 Disk Galaxies with Spitzer Photometry and Accurate Rotation Curves*, *AJ* **152**, 157 (2016), doi:10.3847/0004-6256/152/6/157.
22. 2015. M. den Heijer *et al.*, *The stellar mass Tully–Fisher relation of early-type galaxies*, *A&A* **581**, A98 (2015), doi:10.1051/0004-6361/201525889.
23. 2013. T. Into and L. Portinari, *New colour-mass-to-light relations for stellar population synthesis*, *MNRAS* **430**, 2715 (2013), doi:10.1093/mnras/stt071.
24. 2017. H. Desmond, *The Tully–Fisher and mass-discrepancy–acceleration relations predict the same dark matter distribution*, *MNRAS* **472**, L35 (2017), doi:10.1093/mnrasl/slx147.
25. 2016. S.S. McGaugh, F. Lelli and J.M. Schombert, *Radial Acceleration Relation in Rotationally Supported Galaxies*, *Phys. Rev. Lett.* **117**, 201101 (2016), doi:10.1103/PhysRevLett.117.201101.
26. 2018. P. Li, F. Lelli, S.S. McGaugh and J.M. Schombert, *Fitting the radial acceleration relation to individual SPARC galaxies*, *A&A* **615**, A3 (2018), doi:10.1051/0004-6361/201731957.
27. 2018. H. Katz *et al.*, *Testing feedback-modified dark matter haloes with galaxy rotation curves: estimation of halo parameters and consistency with ΛCDM scaling relations*, *MNRAS* **480**, 4287 (2018), doi:10.1093/mnras/sty2508.
28. 2016. A. Di Cintio and F. Lelli, *The mass discrepancy-acceleration relation in a ΛCDM context*, *MNRAS* **456**, L127 (2016), doi:10.1093/mnrasl/slv185.
29. 2017. B.W. Keller and J.W. Wadsley, *ΛCDM is consistent with SPARC radial acceleration relation*, *ApJL* **835**, L17 (2017), doi:10.3847/2041-8213/835/1/L17.
30. 2014. J. Schombert and S. McGaugh, *Stellar Populations and the Star Formation Histories of LSB Galaxies*, *AJ* **148**, 77 (2014), doi:10.1088/0004-6256/148/4/77.
31. 1996. J.F. Navarro, C.S. Frenk and S.D.M. White, *The structure of cold dark matter halos*, *ApJ* **462**, 563 (1996), doi:10.1086/177173.
32. 1997. J.F. Navarro, C.S. Frenk and S.D.M. White, *A universal density profile from hierarchical clustering*, *ApJ* **490**, 493 (1997), doi:10.1086/304888.
33. 2014. A.A. Dutton and A.V. Macciò, *Cold dark matter haloes in the Planck era: evolution of structural parameters for Einasto and NFW profiles*, *MNRAS* **441**, 3359 (2014), doi:10.1093/mnras/stu742.
34. 1999. M. Milgrom, *The modified dynamics as a vacuum effect*, *Phys. Lett. A* **253**, 273 (1999), doi:10.1016/S0375-9601(99)00077-8.
35. 1999. R.H. Sanders, *The virial discrepancy in clusters of galaxies in the context of modified Newtonian dynamics*, *ApJ* **512**, 23 (1999), doi:10.1086/306742.
36. 2006. D. Clowe *et al.*, *A direct empirical proof of the existence of dark matter*, *ApJL* **648**, L109 (2006), doi:10.1086/508162.
37. 2017. S. Ettori *et al.*, *Mass profiles of galaxy clusters from X-ray analysis and Emergent Gravity*, *A&A* **600**, A37 (2017), doi:10.1051/0004-6361/201629111.
38. 2017. M.M. Brouwer *et al.*, *First test of Verlinde's theory of Emergent Gravity using weak gravitational lensing measurements*, *MNRAS* **466**, 2547 (2017), doi:10.1093/mnras/stw3192.
39. 2013. M. Cappellari *et al.*, *The ATLAS^{3D} project — XX. Mass-size and mass-σ distributions of early-type galaxies: bulge growth and quenching since $z \sim 2$*, *MNRAS* **432**, 1862 (2013), doi:10.1093/mnras/stt644.
40. 2003. A.J. Romanowsky *et al.*, *A dearth of dark matter in ordinary elliptical galaxies*, *Science* **301**, 1696 (2003), doi:10.1126/science.1087441.
41. 1998. W.J.G. de Blok and S.S. McGaugh, *Testing Modified Newtonian Dynamics with Low Surface Brightness Galaxies: Rotation Curve FITS*, *ApJ* **508**, 132 (1998), doi:10.1086/306381.

 doi:10.20944/preprints202603.2170.v1

42. 2000. S.S. McGaugh, J.M. Schombert, G.D. Bothun and W.J.G. de Blok, *The Baryonic Tully–Fisher Relation*, *ApJL* **533**, L99 (2000), doi:10.1086/312628.
43. 2012. S.S. McGaugh, *The Baryonic Tully–Fisher relation of gas-rich galaxies as a test of ΛCDM and MOND*, *AJ* **143**, 40 (2012), doi:10.1088/0004-6256/143/2/40.